A laboratory-based study correlating the large-strain static constrained modulus to the small-strain shear modulus for clean sands

Ibrahim Lashin, Michael Ghali & Mourad Karray
Department of Civil Engineering – Sherbrooke University, Sherbrooke, Québec, Canada
Mohamed Chekired
Institut de Recherche d'Hydro-Québec, Varennes, Québec, Canada

ABSTRACT
Correlating the stiffness parameters of the soil at opposite ends of the strain spectrum has a unique interest for geotechnical engineers as it may contribute to predicting the bearing capacity from simple field measurements. In particular, the static large-strain constrained modulus (M_{oedo}) could be related to the small-strain shear modulus (G_0) regarding the variation of the physical and mechanical parameters of the soil. In this study, G_0 was estimated from the shear wave velocity (V_s) measurements using the piezoelectric ring-actuator technique (P-RAT) on six different clean sands with different characteristics. The corresponding M_{oedo} values were derived from the properties of the resulted stress-strain curves. Based on the analyses of results obtained, correlations between M_{oedo} and V_s and/or G_0 were established considering the different physical characteristics. These relationships may be utilized to predict soil moduli at large deformations from in-situ V_s measurements.

RÉSUMÉ
Corréler les paramètres de rigidité du sol à différents intervalles de déformation a un intérêt particulier pour les ingénieurs géotechniciens, car il peut contribuer à la prédiction de la capacité portante d'un sol à partir de simples mesures sur terrain. En particulier, le module œdométrique à grande déformation (M_{oedo}) pourrait être lié au module de cisaillement à faible déformation (G_0) en ce qui concerne la variation des paramètres physiques et mécaniques du sol. Dans cette étude, G_0 a été estimée à partir des mesures de vitesse d'onde de cisaillement (V_s) en utilisant la technique des anneaux piézoélectriques actuateurs (P-RAT) sur six différents sables propres aux caractéristiques différentes, alors que les valeurs de M_{oedo} correspondantes ont été déduites des courbes contrainte-déformation obtenues. L'analyse des résultats obtenus a permis d'établir des corrélations entre M_{oedo} et V_s et/ou G_0 en tenant compte des différentes propriétés physiques. Ces relations peuvent être utilisées pour prédire le module du sol à grandes déformations à partir de mesures de V_s in situ.

1 INTRODUCTION

Large- and small-strains of the subsoil are key parameters in the geotechnical designs. Researches customarily examine the large-strain behavior using traditional triaxial tests in drained conditions, and oedometer tests as well, whereas, the short-term behaviors are mostly estimated using geophysical methods. Also, investigations on the behavior of soil in the small-strain range (ε <10^{-3}) are substantial in many geotechnical applications (such as; liquefaction assessments where the small stress-strain properties of granular soils may be considered elastic-linear). The small strain shear modulus, G_o, can be evaluated either from in-situ (Campanella et al.1986; Hryciw 1990) or laboratory techniques (Hardin and Richart 1963; Brignoli et al. 1996; Karray et al. 2015) then theoretically calculated from the shear wave velocity measurements, V_s, as ($G_o=\rho V_s^2$, where ρ is the density of the soil).

In the early 1970s, researchers started to involve G_o in modeling the dynamic behavior of the soil (e.g., Seed and Idris 1970), then later, several studies demonstrated its important involvement on the seismic hazard studies (e.g., Riepl et al. 2000; Louie 2001; Wang and Hao 2002; Thompson et al. 2010; Theilen-Willige 2010). Therefore, the small strain shear modulus is fundamental in analyzing the dynamic response of the soil for various geotechnical designs, such as; the subsoils located beneath foundations in active seismic areas, shoring systems, deep excavations beside existing buildings, tunneling, pile foundations, seismic soil-structure interactions, and soil liquefaction potentials (Robertson et al. 1995; Kramer 1996; Ishihara 1996; Youd et al. 2001; Bui 2009). Moreover, numerous researches have focused intensively on employing G_o into the static geotechnical applications such as the static foundation engineering designs (e,g, Imai and Yoshimura 1976; Eberhart-Phillips et al. 1989; Sully and Campanella 1995; and Pyrak-Nolte et al. 1996). Other studies proposed empirical correlations of G_o with the ultimate bearing capacity of soils. Also, Turker (2004) developed an explicit expression for the allowable bearing pressure using V_s.

On the other hand, the large deformation behavior usually represented by elasticity modulus (E) which defined as the ability of a material to resist the excessive deformation during loading. In this study, the oedometer constrained modulus (M_{oedo}) was utilized to represent the elasticity in oedometer conditions. The rigid walls of the oedometer cell prevent the radial deformation, which leads to a vertical (uniaxial) compressive strain test.

Although only axial stresses were applied to the tested soil specimen, there is developed radial stresses due to the laterally constrained condition. Therefore, the results of one-dimensional consolidation oedometer test are typically considered acceptable for foundation designs and the laboratory modeling of soil-foundation behaviors (e.g., Lenk 2009).

Research works investigated the correlation between dynamic (small-strain) and static (large-strain) stiffness moduli (e.g., Salgado et al. 2000, Wichtmann and Triantafyllidis 2006; Wichtmann et al. 2017). Wichtmann et al. (2017) investigated the results of resonant column, triaxial, and oedometer compression tests to evaluate the small-strain shear modulus (G_o) and constrained modulus (M_{oedo}) as well. They also developed empirical formulas correlating G_o to M_{oedo} by examining reconstituted and premixed sand specimens of similar particle shape characteristics, different uniformity coefficient (C_u), and different mean grain sizes (D_{50}).

In the present laboratory investigation, the authors highlight, display, and discuss the importance of employing G_o into predicting other soil parameters at large deformations. Therefore, the purpose of this study is to establish more reliable and direct correlations between M_{oedo} with V_s and/or G_o of granular soils regarding the development of the relative density (I_d), the soil gradation properties (D_{50} & C_u), and the quantitative shape description (A_{2D}) as well. In details, several specimens from six different natural clean sands with different physical characteristics (particle shape and particle size distribution) were experimented using the piezoelectric ring-actuator (P-RAT) of Karray et al. 2015. The P-RAT results show that G_o can be correlated to M_{oedo} by comparing the V_s measurements with the corresponding stress-strain status during the oedometer tests. The proposed correlations could be used to evaluate the large-strain behaviors beneath the founding level on granular materials from a simple direct (in-situ) measurement of the ground shear wave velocity which represents the real behavior of the subsoil without any disturbance. Also, for a limited budget project, which exposed to dynamic loads or located in active seismic areas, the current proposals could be employed with inexpensive tests such as oedometer test, allowing for an acceptable conservative design. Therefore, the achievements of this research may be considered helpful to the foundations' design process.

2 TESTING EQUIPMENT

Piezoelectric elements with different geometries (i.e., strips, plates, discs, etc.) were widely used as laboratory techniques for measuring wave propagation in media (e.g., Brignoli et al. 1996; Yama-shita et al. 2009; Clayton 2011), they proved the ability to transfer electric pulses into vibrations and vice versa. The current experimental investigation was conducted using the piezoelectric ring-actuator technique (P-RAT), which developed at the Université de Sherbrooke (e.g., Gamal El-Dean 2007; Ethier 2009; Éthier et al. 2011; Karray et al. 2015 Elbeggo et al., 2019), to advance the interpretation method of output signals during measurement of soil shear wave velocity. It was developed to minimize the difficulties associated with other techniques of laboratory V_s measurements such as Bender Element (BE) or Resonant Column (RC). The P-RAT offers the possibility to avoid penetrating the tested specimen with the sensors that may be needed in the BE method to transmit the shear strains. Also, P-RAT could be easily incorporated into several traditional geotechnical apparatuses such as triaxial and oedometer. In this study, the P-RAT incorporated into the oedometer apparatus. Thus, both M_{oedo} and V_s can be recorded simultaneously under the same boundaries and stress conditions.

The utilized P-RAT (described in detail by Karray et al., 2015; Elbeggo et al., 2019) consists of two piezoelectric rings representing both emitter and receiver sensors. A small bishop oedometer type cell with a diameter, d=63 mm, and height, h=18 mm, was used through the current study. The soil specimen is installed in the oedometer cell, and the piezoelectric emitter element was fastened to the bottom of the cell, while, the receiver element was fastened to top loading cap.

The emitter can transmit the shear wave by converting the electrical voltage inputs of several signals and frequencies to cover frequency bands lower and above the fundamental frequency of the system and characterize the emitter-receiver dynamic system. The receiver diffuses the resulted data to the acquisition card. An interpretation method was adopted by projecting the signals from the time domain in a frequency domain to locate the frequency range over which the energy is located. On this range, the phase shift between transmitted and received signal should be corrected by the difference of the experimental phase onto the theoretical phase. The theoretical phase shift curve was representing the transfer function (the contribution of the sensors) and was determined by a tip-to-tip test. As a result, the different corrected experimental dispersion curves of different signals under the same testing conditions refer to a constant value of the real shear wave velocity. In other words, the shear wave velocity is independent of the phase or the frequency content of the transmitted signal.

3 TESTED MATERIAL

P-RAT tests were conducted on sands of different physical and mechanical characteristics (uniformity coefficient, C_u ranging 1.6 - 5; mean grain sizes in the range 0.217mm ≤ D_{50} ≤ 0.6mm; several e_{max} - e_{min} & various shape characteristic as well). These natural sands have a percentage of fines, F_C% ≤ 5.4%. Figure 1 represents the particle size distribution for the six tested sands.

The image analyses technique was considered for the soil shape classification in the current study (described in detail by Ghali et al., 2018 & 2019). Figure 2 shows scaled images of the six soils tested. A light stereomicroscope (Leica MZFL-III fluorescence stereo-zoom microscope) was employed for producing the scaled images. Ghali et al., 2018 indicated that the two-

dimensional angularity (A_{2D}) may represent the large (particle form size) and intermediate (corner conditions) scales of particle shape and it can be estimated according to the relationship provided by (Miura et al., 1997, Das et al., 2012 and Ghali et al., 2019) and based on the modified charts of Lees (1964a & 1964b), as shown in Figure 3. The characteristics of all tested sands (G_s, D_{50}, C_u, e_{max}, e_{min}, and F_c%), and the quantitative (A_{2D}) values & shape descriptions are listed in Table 1.

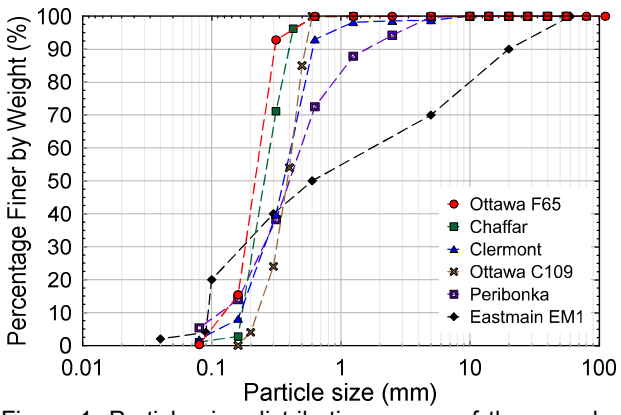

Figure 1. Particle size distribution curves of the granular samples tested.

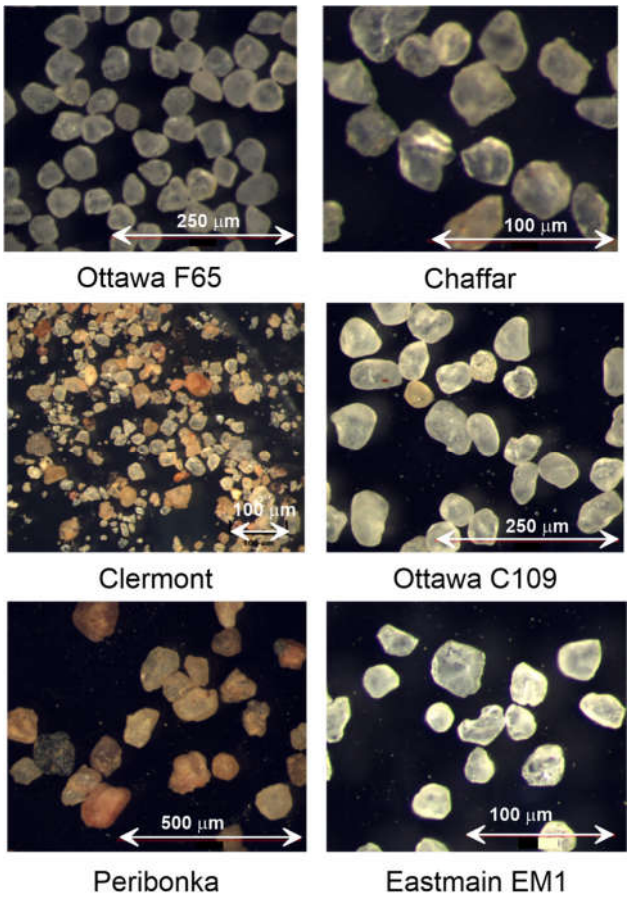

Figure 2. Digital images for tested granular materials

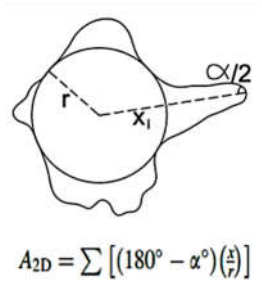

$$A_{2D} = \sum \left[(180° - \alpha°) \left(\frac{x}{r} \right) \right]$$

Figure 3. Definition used for predicting the average A_{2D} modified after (Miura et al., 1997 & Ghali et al., 2018).

Table 1. List characteristics of sands tested in this study

Soil Type	Ottawa F65	Chaffar	Clermont	Ottawa C109	Perib-onka	EM1
G_s	2.66	2.69	2.72	2.65	2.7	2.69
D_{50}	0.217	0.270	0.350	0.380	0.411	0.600
C_u	1.68	1.5	2	1.83	4	5
e_{max}	0.820	0.990	0.990	0.900	0.850	0.820
e_{min}	0.558	0.580	0.502	0.480	0.350	0.410
F_c (%)	0	1	0.2	0	5.4	2
A_{2D}	443	662	737	276	616	714
Shape	SR-SA	SA	SA-A	SR	SA	SA-A

SR = Subround; SA = Subangular; SR – SA = Subround to Subangular; SA – A = Subangular to Angular & A = Angular.

4 METHODOLOGY AND MEASUREMENTS

A large number of laboratory tests on the different clean sand samples were carried out to determine the stress-strain (σ'_v- ε) curves in oedometer conditions that can be used to determine the static constrained modulus (M_{oedo}) in question. The development of the vertical strain (ε) with the applied vertical stress (σ'_v) in kPa under different initial densities for the soils tested were recorded. For example, Figure 4-a shows the stress-strain (σ'_v- ε) curves for Clermont sand tested under three different initial relative densities (I_{di} = 6 to 60%). The variation of the applied vertical stress (σ'_v) and the measured corresponding vertical strain (ε) for the different soils can be approximated in the form of a second-order polynomial function as:

$$\sigma'_v = a.\varepsilon_v^2 + b.\varepsilon_v + c \qquad [1]$$

where a, b and c are the correlative parameters.

Theoretically, the constrained modulus can be determined at any stress state by differentiating the polynomial function (Eq. 1) as the constrained modulus is corresponding to the slope of the tangent on the stress-strain curve, as indicated in Figure 4-a:

$$M_{oedo} = \frac{\partial \sigma'_v}{\partial \varepsilon} \qquad [2]$$

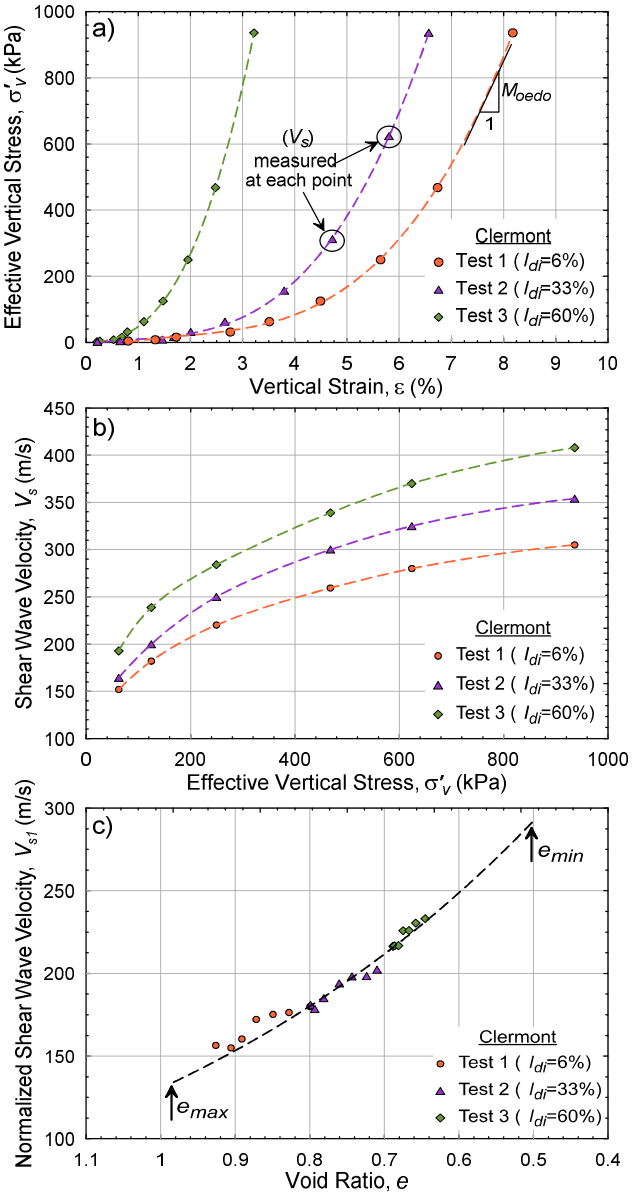

Figure 4. Results of Clermont Sand: b) V_s as a function of the vertical applied stress; c) V_{s1} as a function of void ratio.

On the other hand, the various values of shear wave velocity (V_s) of the six tested soils were recorded for all strain levels under several stress states and different initial relative density values. Figure 4-b represents the relation between V_s and σ'_v for tests performed on Clermont sand under three different I_{di} values. It was observed that V_s is a function of σ'^n_v, where $n \approx 0.25$, in agreement with a majority of researches in the literature (e.g., Hardin and Richart, 1963; Hardin and Black, 1966; Hardin Drnevich 1972). Therefore, V_s values were routinely stress normalized following numerous researchers (e.g., Robertson et al., 1992; Youd et al. 2001; Karray et al. 2011; Hussien and Karray 2016) as:

$$V_{s1} = V_s \left(\frac{P_a}{\sigma_v'} \right)^{0.25} \quad [3]$$

where V_{s1} is the stress-normalized shear wave velocity, and P_a is atmospheric reference pressure of 100 kPa (in the same unit as σ'_v). The variation of V_{s1} as a function of the void ratio (e) for Clermont sand is plotted in Figure 4-c. It is clearly observed that the void ratio is the major parameter controlling the variation of the normalized shear wave velocity (e.g., Karray et al., 2015) since the normalized shear wave velocities of specimens of the same soil (Clermont sand) tested under different initial relative densities (I_{di} = 6 to 60 %) are located on the same trend.

5 RESULTS AND DISCUSSION

5.1 Normalized Shear Wave Velocity (V_{s1})

Normalized V_{s1} values of all tested sands were plotted against the void ratios in Figure 5-a, showing that the values of V_{s1} for all tested specimens ranging between 100 and 325 m/s. Also, it is worth mentioning that the variation of V_{s1} between the loosest and the densest state of the same soil was not more than or around 130 m/s. In other words, the normalized shear wave velocities of specimens of the same granular soil tested at different void ratios collapse onto a relatively narrow range; this observation agrees with previous experimental and field studies of shear wave velocities on granular soils (e.g., Karray et al. 2010, Hussien and Karray 2016). Figure 5-a also demonstrates that the higher the C_u of the tested soil, the lower the obtained normalized shear wave velocity (V_{s1}). This behavior was also observed in some previous studies (e.g., Iwasaki and Tatsuoka 1977, Wichtmann and Triantafyllidis 2006). In this study, an exponential trend was assumed for (V_{s1}–e) relation, in accordance with Karray et al., 2015, the authors performed multi-regression analyses to represent the relationship as:

$$V_{s1} = 380 D_{50}^{0.025} C_u^{-0.09} \exp^{\left[\frac{33}{100000} A_{2D}\right]} \exp^{[-1.07e]} \quad [4]$$

The trending behavior of Eq. 4 with the variation of D_{50}, C_u, and A_{2D} values was also illustrated in Figure 5-a.

Based on a compilation of laboratory and field data, Hussien and Karray (2016) proposed an equation to estimate the value of the normalized shear wave velocity (V_s) from the soil relative density (I_d) and the effective mean diameter (D_{50}):

$$V_{s1} = 5.68[\ln(D_{50}) + 4.84](I_d\% + 25)^{0.5} \quad [5]$$

The (V_{s1}-e) data in Figure 5-a was replotted in Figure 5-b in term of the variation of V_{s1} with the relative density, the upper and the lower limits computed from Hussien and Karray equation (Eq. 5) were plotted as references. Obviously, from Figure 5-b, most of the V_{s1} values determined in the current laboratory tests collapse onto the range provided by Eq.5.

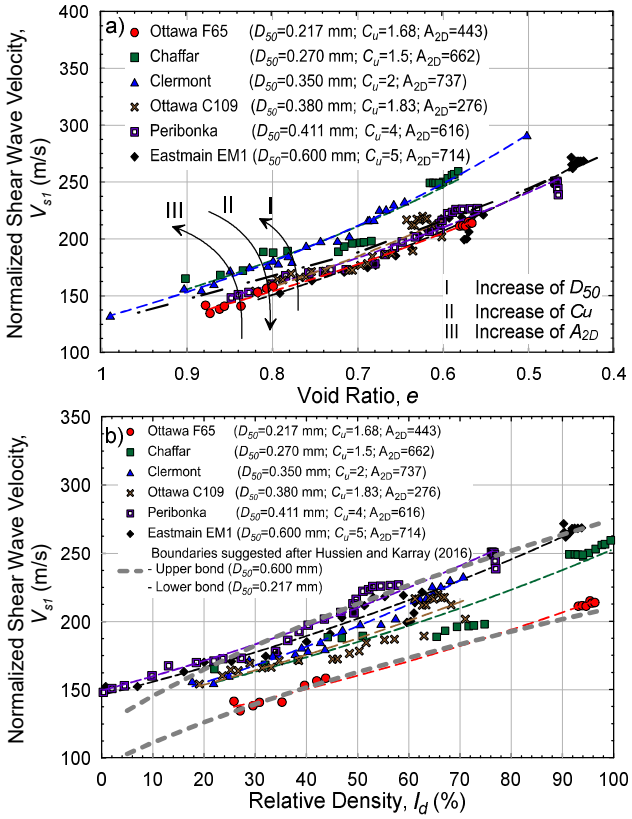

Figure 5. a) Normalized shear wave velocity (V_{s1}) as a function of void ratio; b) Normalized shear wave velocity (V_{s1}) as a function of relative density.

5.2 Small-Strain Shear Modulus (G_o)

The small-strain shear modulus is theoretically calculated as $G_o=\rho V_s^2$, where ρ is the density of the material. The obtained results of G_o are normalized concerning the applied vertical stress [$G_o(100/\sigma'_v{}^{0.5}$] and plotted in MPa against the void ratio (e) as shown in Figure 6.

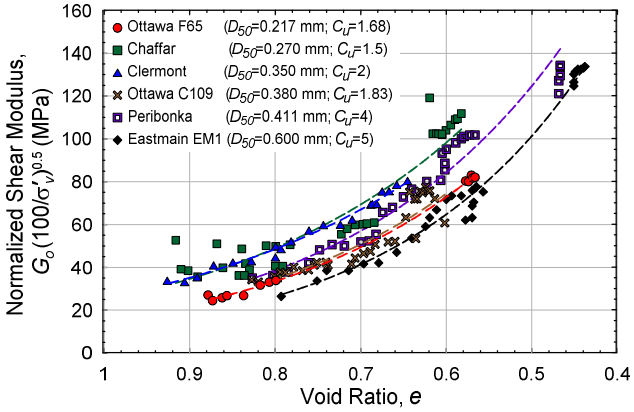

Figure 6. Normalized shear modulus as a function of void ratio.

It is clear that the normalized G_o increases with decreasing of void ratio and the higher the C_u of the soil, at a given void ratio, the lower the normalized shear modulus G_o, which seems logical and agrees with the literature (e.g., Wichtmann et al., 2017).

5.3 Large-strain constrained modulus (M_{oedo})

The constrained modulus determined at different stress states of the tested soils are normalized concerning the applied vertical stress; where the normalized constrained modulus was calculated as [M_{oede} $(100/\sigma'_v{}^{0.5}$], then the normalized values in MPa were plotted against the void ratio (e) as shown in Figure 7.

Ohde (1951) suggested a value of normalized constrained modulus ranged between 10 to 75 MPa for granular soils, and the obtained values of all tested granular soils show good agreement with this range. Figure 7 also indicates that the normalized M_{oedo} increases with decreasing the soil void ratio.

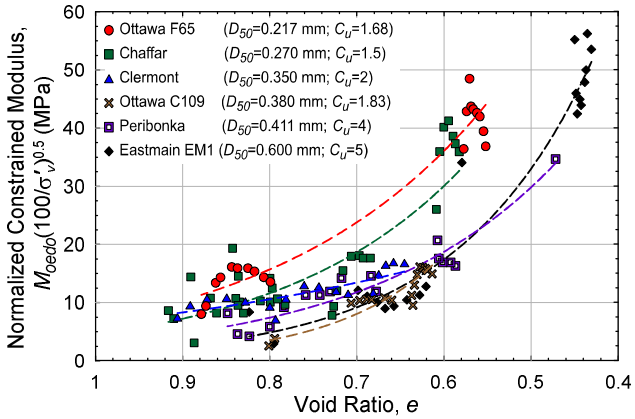

Figure 7. Normalized constrained modulus as a function of void ratio.

5.4 (M_{oedo}/G_o) proposed correlations

The experimental data presented in Figures. 6 & 7 reveals the presence of observable correlations between M_{oedo}/G_o with the development of I_d, as shown in Figure 8. It is clear that all curves of the tested soils have exponential trends. The results presented in Figure 8 show that the correlation between the M_{oedo}/G_o and the soil relative density can be expressed as:

$$\frac{M_{oedo}}{G_o} = A\exp^{[B(I_d\%)]} \qquad [6]$$

where the fitting parameters, A ranges from 0.066 to 0.445, and B ranges from 0.0011 to 0.0183. Table 2 shows the values of the fitting parameters A and B for all tested soils.

Subsequently, depending on the soil gradation and particles shape characteristics listed in table 1, particle size distribution curves showed in Figure1 and the values of the parameters A and B for all tested soil represented

in table 2; the geotechnical designers could use these data as a guide to estimate the parameters A and B for clean sands. In the ongoing efforts to provide a more rational method of determining the empirical parameters (A and B) a plan of a comprehensive experimental investigation is set, and it will be soon conducted employing a variety of sands with different particle shape, fines content, and grading characteristics.

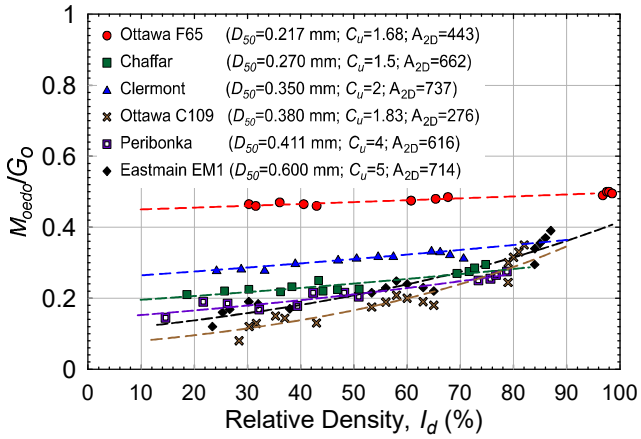

Figure 8. M_{oedo}/G_0 as a function of relative density

Table 2. Fitting parameters of Eq.6

Soil Type	Ottawa F65	Chaffar	Clermont	Ottawa C109	Perib-onka	EM1
A	0.445	0.227	0.254	0.066	0.140	0.104
B	0.0011	0.0059	0.0040	0.0183	0.008	0.0140

6 CONCLUSIONS

This paper presents the results of experimental work carried out on six different clean sands to establish the correlation between the static large-strain stiffness constrained modulus (M_{oedo}) and the shear wave velocity (V_s) and/or the small-strain shear modulus (G_o). For clean sands, a new correlation of V_{s1} and e is proposed and the relations of M_{oedo} – e and G_o – e have been reformulated gathering M_{oedo}/G_o to the relative density (I_d). It is observed that, at a given void ratio, V_{s1} was positively related to D_{50} and A_{2D} while negatively related to C_u. Also, M_{oedo}/G_o ratio, at a given I_d value, is significantly influenced by the variation of the physical parameters; such as D_{50}, A_{2D}, and C_u.

REFERENCES

Brignoli, E.G.M., Gotti, M., and Stokoe, K.H. 1996. Measurement of shear waves in laboratory specimens by means of piezoelectric transducers. *Geotechnical Testing Journal*, 19(4): 384–397.

Bui, M.T., 2009. Influence of some particle characteristics on the small strain response of granular materials. *Phd. dissertation*, University of Southampton.

Campanella, R. G., Robertson, P. K., and Gillespie, D. 1986. Seismic cone penetration test. *Use of in situ tests in geotechnical engineering,* ASCE, 116–130.

Clayton, C. R. I. 2011. Stiffness at small strain: research and practice. *Géotechnique,* 61(1), 5-37.

Das, B.M., Sivakugan, N., and Atalar, C. 2012. Maximum and minimum void ratios and median grain size of granular soils: their importance and correlations with material properties. *In proceedings of the 3rd International Conference on New Developments in Soil Mechanics and Geotechnical engineering*.

Eberhart-Phillips, D., D.-H. Han, and M.D. Zoback 1989. Empirical relationships among seismic velocity, effective pres-sure, porosity, and clay content in sandstone. *Geophysics,* 54, 82-89.

Elbeggo, D., Hussien, M.N., Ethier, Y., and Karray, M., 2019. Robustness of the P-RAT in the Shear-Wave Velocity Measurement of Soft Clays. *Journal of Geotechnical and Geoenvironmental Engineering*, Vol. 145(5). DOI 10.1061/(ASCE)GT.1943-5606.0002017

Éthier, Y., Karray, M., Lefebvre, G., 2011. Simulations of elastic wave propagation using FLAC to optimize the measurement of shear wave velocity in the laboratory, *Proceedings of the 2nd international FLAC/DEM symposium*, Continuum and distinct element numerical modeling in geomachanics, Merbourne, Australia: 519-527.

Ethier, Y.A. 2009. La mesure en laboratoire de la vitesse de propagation des ondes de cisaillement. PhD Thesis, Université de Sherbrooke.

Ghali, M., Chekired, M., and Karray, M., 2018. "Framework to improve the correlation of SPT-N and the geotechnical parameters in sands" *ActaGeotechnica*, ISSN: 1861-1133.

Ghali, M., Chekired, M., and Karray, M., 2019. "A laboratory-based study correlating cone penetration test resistance to the physical parameters of uncemented sand mixtures and granular soils" *Engineering Geology*, Vol (255):11 – 25.

GamalEl-Dean. 2007. Development of a new piezoelectric pulse testing device and soil characterization using shear waves. PhD Thesis, Université de Sherbrooke.

Hardin, B.O., and Richart, J.F.E. 1963. Elastic wave velocities in granular soils. *Journal of the Soil Mechanics and Foundations Division*, 89 : 33–63.

Hardin BO, Black WL. 1966. Sand stiffness under various triaxial stresses. J*ournal of the Soil Mechanics and Foundations Division*; 92(SM2):27–42.

Hardin, B.O., and Drnevich, V.P. 1972. Shear modulus and damping in soils: measurement and parameter effect. J*ournal of the Soil Mechanics and Foundations Division*, 96(SM7): 667–692.

Hussien, M. N., & Karray, M., 2016. Shear wave velocity as a geotechnical parameter: an overview. *Canadian Geotechnical Journal*, 53(2), 252-272.

Hryciw, R. D. 1990. Small-strain-shear modulus of soil by dilatometer. *Journal of Geotechnical Engineering,* ASCE, 116(11), 1700-1716.

Imai, T., and M. Yoshimura 1976. The relation of

mechanical properties of soils to P- and S-wave velocities for soil ground in Japan. *Urana Research Institute*, OYO Corporation, Tokyo, Japan.

Ishihara, K. 1996. Soil behaviour in earthquake geotechnics. Clarendon Press; Oxford University Press.

Iwasaki, T., & Tatsuoka, F. 1977. Effects of grain size and grading on dynamic shear moduli of sands. *Soils and foundations,* 17(3), 19-35.

Karray, M., Lefebvre, G., Ethier, Y. and Bigras, A. 2010. Assessment of deep compaction of the Péribonka dam foundation using "modal analysis of surface waves" (MASW). *Canadian Geotechnical Journal*, 47(3), pp.312-326.

Karray, M., Lefebvre, G., Ethier, Y., and Bigras, A., 2011. Influence of particle size on the correlation between shear wave velocity and cone tip resistance. *Canadian Geotechnical Journal,* 48(4): 599–615. doi:10.1139/t10-092.

Karray, M., Ben Romdhan, M., Hussien, M.N., and Éthier, Y. 2015. Measuring shear wave velocity of granular material using the piezoelectric ring-actuator technique (P-RAT). *Canadian Geotechnical Journal*, 52(9): 1302–1317.

Kramer, S.L. 1996. Geotechnical earthquake engineering. Pearson Education India.

Lees, G. 1964a. A new method for determining the angularity of particles. *Sedimentology*. Vol., 3, pp. 2-21.

Lees, G. 1964b. The measurement of particle shape and its influence in engineering materials. *British Granite Whinstone Federation*. Vol., 4, No. 2, pp. 17-38.

Lenk, P. 2009. Modelling of Primary Consolidation. *Slovak Journal of Civil Engineering*, 26-37.

Louie, J. N. 2001. Faster, better: shear-wave velocity to 100 meters depth from refraction microtremor arrays. *Bulletin of the Seismological Society of America*, 91(2), 347-364.

Miura, K., Maeda, K., Furukawa, M., and Toki, S. 1997. Physical Characteristics of sands with different primary proper-ties. *Soils and Foundations*, 37(3): 53 - 64.

Ohde, J. 1951. Grundbaumechanik (in German), *Huette*, BD. III, 27. Auflage

Pyrak-Nolte, L.J., Roy S., and Mullenbach B.L. 1996. Interface waves propagated along a fracture. *Journal of Applied Geophys*. 35, 2-3, 79-87.

Riepl, J., Zahradn`ık, J., Plicka, V. P., and Bard, Y. 2000. About the Ef-ficiency of Numerical 1-D and 2-D Modelling of Site Effects in Basin Structures. *Pure Appl. Geophys.*, 157, 319–342.

Robertson, P.K., Woeller, D.J., Kokan, M., Hunter, J., Luternaur, J., 1992. Seismic techniques to evaluate liquefac-tion potential. *In Proceedings of the 45th Canadian geotechnical conference*, Toronto, Ont., pp 5-1–5-9.

Robertson, P.K., Sasitharan, S., Cunning, J.C., and Sego, D.C. 1995. Shear-wave velocity to evaluate in-situ state of Otta-wa sand. Journal of Geotechnical Engineering, 121(3): 262–273.

Salgado, R., Bandini, P., & Karim, A. 2000. Shear strength and stiffness of silty sand. *Journal of Geotechnical and Geoenvironmental Engineering*, 126(5), 451-462.

Seed, H. B. and Idriss, I. M. 1970. Soil Moduli and Damping Factors for Dynamic Response Analyses Research Report EERC 7010, *Earthquake Engineering Research Center*, University of California, Berkeley, Calif.

Sully, J.P., and R.G. Campanella 1995. Evaluation of in situ anisotropy from crosshole and downhole shear wave veloci-ties measurements. *Geotechnique,* 45, 2, 267-282.

Theilen-Willige, B. 2010. Detection of local site conditions influencing earthquake shaking and secondary effects in Southwest-Haiti using remote sensing and GIS-methods. *Natural Hazards and Earth System Sciences,* 10, 1183–1196.

Thompson, E. M., Baise, L. G., Kayen, R. E., Tanaka, Y., and Tanaka, H. 2010. A geostatistical approach to mapping site response spectral amplifications. *Engineering Geology*, 114, 330–342, 2010.

Turker, E. 2004. Computation of ground bearing capacity from shear wave velocity. In: D. Bergman et al. (eds.), Contin-uum Models and Discrete Systems *Kluwer Academic Publishers*, Netherlands, 173-180.

Wang, S. and Hao, H. 2002. "Effects of random variations of soil properties on site amplification of seismic ground motions." *Soil Dynamics and Earthquick Engineering*, 22, 551–564, 2002

Wichtmann T, Triantafyllidis T. 2006. On the correlation of oedometric and dynamic stiffness of non-cohesive soils (in German). *Bautechnik*;83(7):482–91.

Wichtmann, T., Kimmig, I., & Triantafyllidis, T. 2017. On correlations between "dynamic"(small-strain) and "static" (large-strain) stiffness moduli – An experimental investigation on 19 sands and gravels. *Soil Dynamics and Earthquake Engineering*, 98, 72-83.

Yamashita, S., Kawaguchi, T., Nakata, Y., Mikami, T., Fujiwara, T., & Shibuya, S. 2009. Interpretation of international parallel test on the measurement of Gmax using bender elements. *Soils and foundations*, 49(4), 631-650.

Youd, T.L., Idriss, L.M., Andrus, R.D., Arango, I., Castro, G., Christian, J.T., et al. 2001. Liquefaction resistance of soils: summary report from the 1996 NCEER and 1998 NCEER/NSF workshops on evaluation of liquefaction resistance of soils. *Journal of Geotechnical and Geoenvironmental Engineering*, 127(10): 817–833.